Two-Stage Maximum Likelihood Estimation (TSMLE) for MT-CDMA Signals in the Indoor Environment

Quazi Mehbubar Rahman

Department of Electrical & Computer Engineering, Queen's University, Kingston, ON, Canada K7L 3N6
Email: rahman@post.queensu.ca

Abu B. Sesay

Department of Electrical & Computer Engineering, University of Calgary, AB, Canada T2N 1N4
Email: sesay@enel.ucalgary.ca

Mostafa Hefnawi

Department of Electrical & Computer Engineering, Royal Military College of Canada, ON, Canada K7K 7B4
Email: hefnawi-m@rmc.ca

This paper proposes a two-stage maximum likelihood estimation (TSMLE) technique suited for multitone code division multiple access (MT-CDMA) system. Here, an analytical framework is presented in the indoor environment for determining the average bit error rate (BER) of the system, over Rayleigh and Ricean fading channels. The analytical model is derived for quadrature phase shift keying (QPSK) modulation technique by taking into account the number of tones, signal bandwidth (BW), bit rate, and transmission power. Numerical results are presented to validate the analysis, and to justify the approximations made therein. Moreover, these results are shown to agree completely with those obtained by simulation.

Keywords and phrases: code division multiple access, indoor fading channel, OFDM, maximum likelihood estimation.

1. INTRODUCTION

High-data-rate multimedia communications is one of the challenges currently being addressed in the research domain for the upcoming next generation wireless systems [1, 2]. Although the third generation (3G) systems (www.3gtoday.com) are supporting a maximum data rate of 153 kbps (CDMA2000) and 384 kbps (WCDMA) for voice and data applications, and 2.4 Mbps for data-only (CDMA 2000 1xEV-DO) applications, transmission rate for combined voice and data applications for the future generation systems is expected, and needed to be much higher. Consequently, researchers are exploring different schemes for high-data-rate applications. In this regard, multicarrier modulation schemes [3] such as multitone code division multiple access (MT-CDMA) system [4] are getting special attention [5]. MT-CDMA, a combination of orthogonal frequency division multiplexing (OFDM) and direct-sequence spread-spectrum (DS-SS) modulation, provides both high-data-rate transmission and multiple-access capabilities. Several research studies have developed MT-CDMA-based efficient schemes to combat different adverse effects, such as multiple-access in-

terference (MAI) and multipath fading. However, no optimal detection technique has yet been devised. In this paper, we are proposing two-stage maximum likelihood estimation (TSMLE) as one of the probable solutions for the problem of optimal detection of MT-CDMA signals. The first stage of the TSMLE-based receiver performs the channel estimation, considering that either the received symbol or the estimate of the received symbol is known, while the second stage uses this estimated channel information to estimate the next symbol.

The theory of TSMLE was first proposed by Sesay [6] as an alternative to maximal ratio combining (MRC) of predetection type. MRC is a scheme that first weighs the individual diversity signals according to their signal-to-noise ratios (SNR), aligns their phases, and then sums them. Phase alignment requires fast and stable phase tracking loops for the wireless radio channel. But, due to several reasons, such as oscillator phase instability, mobility of transmitter and/or receiver, multipath fading, stable and fast tracking of the phase becomes very difficult; it becomes nearly unattainable when high-speed data applications are considered.
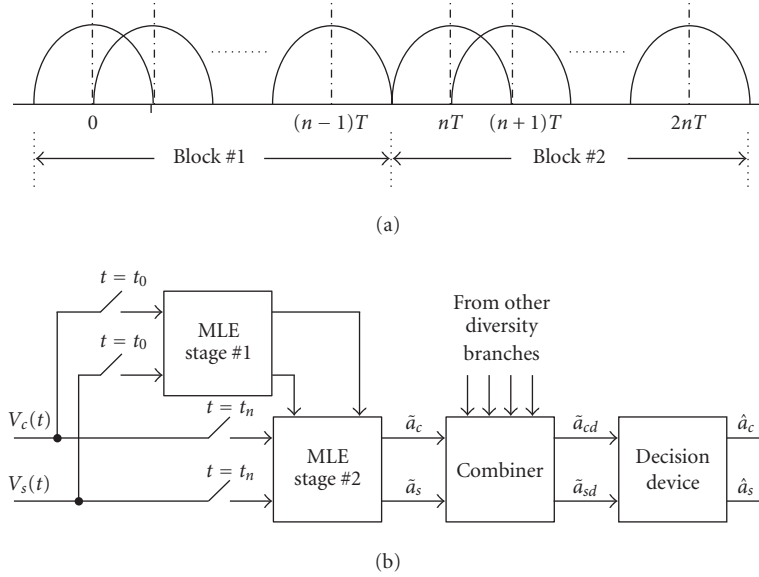
(a)

(b)

FIGURE 1: Two-stage maximum likelihood receiver: (a) the signaling format, (b) the receiver block diagram.

In the operation of TSMLE, the incoming data in the quadrature branches is divided into blocks of sufficient length, each of which is preceded by a reference symbol, known to the receiver, as shown in Figure 1a. The blocks are chosen such that the channel impulse response in each of these block intervals remains unchanged. As shown in Figure 1b, a detector follows the TSMLE. The reference interval of each block is sampled and maximum likelihood (ML) estimates of the quadrature channel gains are computed. Here, all channel amplitudes and phase variations are lumped into the quadrature gains, which are considered to be Gaussian processes, and ML methods are used for their estimation. Next, given the gain estimates, each data interval is sampled and ML estimates of the data bit values are computed. These estimated data bits are decoded at the output of the decoder according to their signs.

TSMLE provides manifold advantages. As pointed out in [7, 8], since quadrature gain estimation, given by TSMLE operation, is equivalent to phase estimation, the nonlinear loop requirement of phase tracking is eliminated. It has been shown in [9] that the complete TSMLE scheme is relatively simpler to implement than other reported schemes with comparable performance [7, 8, 10, 11, 12, 13, 14]. Besides, in the high bit rate environment, the overhead encountered from the reference symbols in TSMLE is reasonably small [6]. Capitalizing these advantages of TSMLE technique lets us find out further the reasons behind using this technique for MT-CDMA-based system. In [9] Sesay showed that the adaptation of adaptive TSMLE-based receiver must be achieved within one symbol period for efficient performance. In other words, larger symbol duration will result in better adaptation for TSMLE-based receiver. MT-CDMA already offers the advantage of generating large symbols due to its parallel transmission nature. As shown in [4, 15], as the

number of tones increases, the BW corresponding to each subchannel gets narrower, and the fading on each subchannel can be considered approximately flat. These conclusions have led us to propose TSMLE-based receiver for MT-CDMA signals. Here, as in [6], accurate timing recovery is assumed and no attempt is made to track phase jitters while all channel effects are considered to be embedded in the gains. Notably, requiring no explicit phase tracking for the received signals, a TSMLE-based receiver could be regarded as a partially coherent system.

In summary, the contribution of this paper includes a proposed receiver structure for MT-CDMA system. A mathematical model is developed to derive the *bit error rate* (BER) performance of this proposed receiver for Rayleigh and Ricean fading indoor channel environments. The theoretical model for the Rayleigh fading channel is validated with simulation results. The analytical model shows the effect of number of tones on the system's performance, and draws a comparison of its BER performance with its corresponding fully coherent receiver performance [4].

The outline of the paper is as follows. The structure of the system is presented in Section 2. In Section 3, the bit error probability of this system is analyzed for an indoor multipath-fading channel in the presence of MAI. Here, both Rayleigh- and Ricean-type fading channels are considered. The analysis is presented in terms of BER. In deriving the BER expressions, inclusion of guard intervals between the tones is not considered since it is clearly shown in [4] that this technique cannot completely suppress different interferences encountered in the system. We consider the situation in which the receiver can acquire time synchronization with the desired signal but not phase synchronization. Section 4 provides some numerical results and points out some possible challenges in this area. Finally conclusions are drawn.
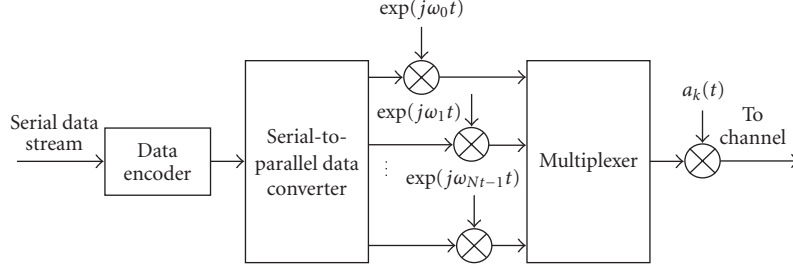
FIGURE 2: Block diagram of MT-CDMA transmitter for user k.

2. SYSTEM MODEL

2.1. Transmitter model

Figure 2 shows the block diagram [4] of an MT-CDMA transmitter for the kth user ($1 \leq k \leq K$) using quadrature phase shift keying (QPSK) modulation. At the transmitter side, a *Gray*-encoded serial QPSK symbol-stream is converted into N_t parallel substreams at a rate of N_t/T streams/s, with symbol duration T. Each of these substreams is then modulated by individual carrier frequencies in each branch. All these carrier frequencies within the symbol duration are orthogonal to each other in such a way that the pth frequency results in $f_p = f_0 + p/T$ with f_0 being the RF frequency. This, essentially, is the OFDM phenomenon that results in overlaps between the spectra associated with different tones; but as long as the orthogonality between these tones is unchanged, the signals carried by each tone can be recovered successfully.

Upon multiplexing different carrier-modulated signals, as shown in Figure 2, multitone signal is obtained. Spectrum spreading is achieved by multiplying the multitone signal with a *pseudonoise* (PN) sequence associated with the user of interest. It is important to note that spectrum spreading does not change the orthogonality property of the multitone signal. The PN sequence $a_k(t)$, associated with user k, has a chip duration of $T_c = T/N_c$, and the sequence is periodic with the sequence length N_c. At the output of the transmitter, the MT-CDMA signal transmitted by user k becomes

$$S_k(t) = \sqrt{2P} \sum_{p=0}^{N_t-1} \mathrm{Re}\left[a_k(t)d_{pk}(t)\exp\left\{-(2\pi jf_pt+j\theta_{pk})\right\}\right],$$

$$(1)$$

where $a_k(t)$ is given by

$$a_k(t) = \sum_{n=0}^{N_c-1} a_k^n P_{T_c}(t - nT_c) \qquad (2)$$

while $d_{pk}(t) = I_{pk}(t) + jQ_{pk}(t)$ is the data symbols associated with pth tone of user k with I_{pk} and Q_{pk} the in-phase and quadrature components, respectively. P is the power associated with each user, which ensures perfect power control, and in turn guarantees that the system is not affected by the near-far problem. The parameter θ_{pk} is a constant phase angle introduced by the modulator of the kth user using the pth

tone. In (2), $a_k^n \in \{1, -1\}$ is the nth bit in the PN-sequence and P_{T_c} is a rectangular pulse of duration T_c.

2.2. Channel model

We assume that the channel between user k transmitter and the corresponding receiver is an indoor multipath-fading channel and is characterized by the complex lowpass equivalent impulse response function of the form

$$h_k(t) = \sum_{l=0}^{L} \beta_{kl} \exp\left(j\gamma_{kl}\right)\delta(t - \tau_{kl}). \qquad (3)$$

The indoor channel model presented in (3) has been discussed in [16] and utilized in [4]. In (3), kl refers to path l of user k with total number of paths L, while γ_{kl} and τ_{kl} are the phases and the propagation delays, respectively. A commonly used assumption is that γ_{kl} and τ_{kl} are independently and uniformly distributed where $\gamma_{kl} \in [0, 2\pi]$ and $\tau_{kl} \in [0, T/N_t]$. All the data bits are considered to be mutually independent and equally likely with ± 1 values.

Finally, for the slow fading channel we can assume that the phase angles, γ_{kl} and θ_{pk}, with other random parameters associated with the channel, do not vary significantly over the duration of two adjacent data symbols. In our analysis we have considered both Rayleigh and Ricean distributed random path gains β_{kl}s. These gains are assumed to be identically distributed and independent for different values of k and l.

The Rayleigh probability density function (PDF) is given by

$$d_{\beta_{kl}} = \begin{cases} \dfrac{r}{\rho_{kl}} \exp\left(-\dfrac{r^2}{2\rho_{kl}}\right), & r \geq 0 \\ 0, & r < 0, \end{cases} \qquad (4)$$

where ρ_{kl}, the variance of β_{kl}, represents the average path power of the lth path associated with user k.

The Ricean PDF is given by

$$d_\beta(r) = \dfrac{r}{\sigma_r^2} \exp\left[-\dfrac{r^2 + S^2}{2\sigma_r^2}\right]I_0\left(\dfrac{rS}{\sigma_r^2}\right), \qquad (5)$$

where $r \geq 0$, $S \geq 0$. The *Ricean parameter*, $R = S^2/2\sigma_r^2$, represents the ratio of the power associated with the direct path
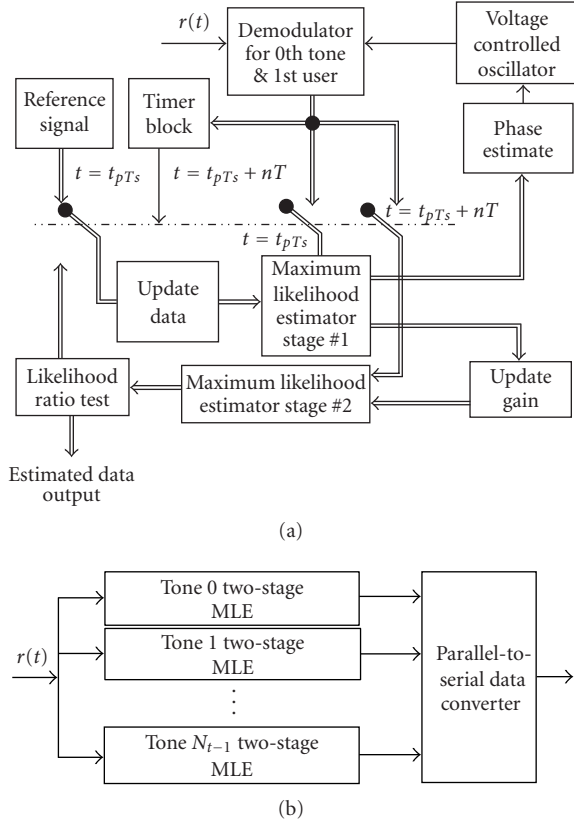
(a)

(b)

FIGURE 3: Block diagrams of the receiver for user 1: (a) tone-0 detector, (b) the complete receiver.

component and the scattered path components in the multipath channel.

In both types of channels, identical distribution of channel coefficients is practically a reasonable assumption for the indoor environment where the transmitter and receiver are closely spaced. In this case, the main reflectors and scatterers result in approximately identical multipath structures [16].

2.3. Receiver model

2.3.1. Basic structure

The proposed block diagram of the receiver for user 1, using a rectangular chip waveform, is shown in Figure 3. Here, the received signal $r(t)$ is given by

$$r(t) = y(t) + n(t), \tag{6}$$

where $y(t)$, the channel-corrupted signal, is given by

$$
\begin{aligned}
y(t) &= \sum_{k=1}^{K} \text{Re} \left\{ S_k(t) * h(t) \right\} \\
&= \sum_{k=1}^{K} \sum_{p=0}^{N_t-1} \sum_{l=1}^{L} \text{Re} \left\{ \sqrt{2P} \beta_{kl} a_k(t - \tau_{kl}) \right. \\
&\quad \times \left[I_{pk}(t - \tau_{kl}) + j Q_{pk}(t - \tau_{kl}) \right] \\
&\quad \left. \times \exp \left\{ -j[2\pi f_q(t - \tau_{kl}) + \theta_{pk} - \gamma_{kl}] \right\} \right\}
\end{aligned}
\tag{7}
$$

and $n(t)$ is an additive white Gaussian noise (AWGN) term of (two-sided) spectral density $N_0/2$ Watts/Hz. In (7), $*$ indicates the convolution operation.

This received signal is demodulated by means of a correlator in each TSMLE receiver corresponding to each tone. In this case, the in-phase and quadrature-phase received signals corresponding to the first user and qth carrier at the correlator output are given by

$$
\begin{aligned}
r_{c1}^q(t) &= \int_0^T r(t) a_1(t) \cos 2\pi f_q t \, dt, \\
r_{s1}^q(t) &= \int_0^T r(t) a_1(t) \sin 2\pi f_q t \, dt.
\end{aligned}
\tag{8}
$$

Substituting (6) and (7) into (8) and after omitting the terms with $2f_0$, the in-phase and quadrature-phase received signals can be written as

$$
\begin{aligned}
r_{c1}^q(t) &= \left[I_{q1}^0 \tilde{G}_{qq1}^{cc} - Q_{q1}^0 \tilde{G}_{qq1}^{sc} \right] + \left[I_{q1}^{-1} G_{qq1}^{cc} - Q_{q1}^{-1} G_{qq1}^{sc} \right] \\
&\quad + \sum_{p=0, \neq q}^{N_t-1} \left\{ I_{p1}^{-1} \left[G_{pq1}^{cc} + G_{pq1}^{ss} \right] + I_{p1}^0 \left[\tilde{G}_{pq1}^{cc} + \tilde{G}_{pq1}^{ss} \right] \right. \\
&\quad \left. + Q_{p1}^{-1} \left[G_{pq1}^{cs} - G_{pq1}^{sc} \right] + Q_{p1}^0 \left[\tilde{G}_{pq1}^{cs} - \tilde{G}_{pq1}^{sc} \right] \right\} \\
&\quad + \sum_{k=2}^{K} \sum_{p=0}^{N_t-1} \left\{ I_{pk}^{-1} \left[G_{pqk}^{cc} + G_{pqk}^{ss} \right] + I_{pk}^0 \left[\tilde{G}_{pqk}^{cc} + \tilde{G}_{pqk}^{ss} \right] \right. \\
&\quad \left. + Q_{pk}^{-1} \left[G_{pqk}^{cs} - G_{pqk}^{sc} \right] + Q_{pk}^0 \left[\tilde{G}_{pqk}^{cs} - \tilde{G}_{pqk}^{sc} \right] + \psi_{q1}^c \right\},
\end{aligned}
\tag{9a}
$$

$$
\begin{aligned}
r_{s1}^q(t) &= \left[I_{q1}^0 \tilde{G}_{qq1}^{sc} + Q_{q1}^0 \tilde{G}_{qq1}^{cc} \right] + \left[I_{q1}^{-1} G_{qq1}^{sc} - Q_{q1}^{-1} G_{qq1}^{cc} \right] \\
&\quad + \sum_{p=0, \neq q}^{N_t-1} \left\{ -I_{p1}^{-1} \left[G_{pq1}^{cs} - G_{pq1}^{sc} \right] - I_{p1}^0 \left[\tilde{G}_{pq1}^{cs} - \tilde{G}_{pq1}^{sc} \right] \right. \\
&\quad \left. + Q_{p1}^{-1} \left[G_{pq1}^{cc} + G_{pq1}^{ss} \right] + Q_{p1}^0 \left[\tilde{G}_{pq1}^{cc} + \tilde{G}_{pq1}^{ss} \right] \right\} \\
&\quad + \sum_{k=2}^{K} \sum_{p=0}^{N_t-1} \left\{ -I_{pk}^{-1} \left[G_{pqk}^{cs} - G_{pqk}^{sc} \right] - I_{pk}^0 \left[\tilde{G}_{pqk}^{cs} - \tilde{G}_{pqk}^{sc} \right] \right. \\
&\quad \left. + Q_{pk}^{-1} \left[G_{pqk}^{cc} + G_{pqk}^{ss} \right] + Q_{pk}^0 \left[\tilde{G}_{pqk}^{cc} + \tilde{G}_{pqk}^{ss} \right] + \psi_{q1}^s \right\},
\end{aligned}
\tag{9b}
$$

where

$$G_{pqk}^{sc} = \sqrt{\frac{P}{2}} \sum_{l=1}^{L} \beta_{kl} \sin(\phi_{pkl}) R_{pqk}^c(\tau_{kl}), \tag{10a}$$

$$\tilde{G}_{pqk}^{sc} = \sqrt{\frac{P}{2}} \sum_{l=1}^{L} \beta_{kl} \sin(\phi_{pkl}) \widehat{R}_{pqk}^c(\tau_{kl}), \tag{10b}$$

$$R_{pqk}^c(\tau_{kl}) = \int_0^{\tau_{kl}} a_1(t) a_k(t - \tau_{kl} + T) \cos 2\pi(p - q) \frac{t}{T} dt, \tag{10c}$$

$$\widehat{R}_{pqk}^c(\tau_{kl}) = \int_{\tau_{kl}}^T a_1(t) a_k(t - \tau_{kl}) \cos 2\pi(p - q) \frac{t}{T} dt, \tag{10d}$$

$$\phi_{pkl} = 2\pi f_p \tau_{kl} - \theta_{pkl} + \gamma_{kl}. \tag{10e}$$

In (9a) and (9b) the G functions are composed of all the channel effects, and are considered to be the channel gain

functions; the superscripts -1 and 0 on the data symbols I and Q are used to represent the previous and current symbols, respectively. In (10a) and (10b), the first superscript in G represents the angular function (s for sine and c for cosine) in the expressions, while the second superscript represents the angular function (s for sine and c for cosine) in R. This R, the *partial cross correlation function* between two PN sequences, is defined in (10c) and (10d) for two different cases. Equation (10e) represents the phase angel of the received signal corresponding to kth user, lth path, and pth tone. Equations (9a) and (9b) can be analyzed as follows. The first term represents the desired signal component for the expected user (i.e., user 1) using the qth tone. The second term is the intersymbol interference (ISI) term due to the partial correlation between the user code and its delayed version. The third term is the intercarrier interference (ICI) term resulting from the other tones of user 1. The ISI due to partial correlation is also present in the third term. The fourth term represents the MAI, which also involves ISI and ICI. The final term is the AWGN term.

2.3.2. TSMLE

First stage

The demodulated signals are sampled at the multitone symbol rate ($t = t_{pTs} + nT$), taking into account the reference time t_{pTs}, which represents the time for p number of QPSK symbols having a duration of T_s each; p being the tone number. For the demodulated data $r_{c1}^q(t)$ and $r_{s1}^q(t)$, we take the samples at every multitone interval T (considering t_{pTs} to be zero, i.e., perfect time synchronization) and compute the MLE of the corresponding channel gain estimates in the first stage. Assuming all the interference and noise terms to be collectively Gaussian in (8) and (9), the sampled quadrature components at the nth interval become

$$
\begin{aligned}
r_{c1,n}^q &= I_{q1,n}\tilde{G}_{qq1,n}^{cc} - Q_{q1,n}\tilde{G}_{qq1,n}^{sc} + \eta_{c1,n}, \\
r_{s1,n}^q &= I_{q1,n}\tilde{G}_{qq1,n}^{sc} - Q_{q1,n}\tilde{G}_{qq1,n}^{cc} + \eta_{s1,n}.
\end{aligned}
\tag{11}
$$

In (11), the superscripts from the data components I and Q have been omitted since they represent the current symbols only. During the start-up period, only known data symbols are present in the received signal. The receiver stores these known data symbols. During this reference period the received samples and these stored symbols are used to generate ML estimates of the quadrature gains. The ML gain estimate in the nth observation interval can be obtained by using standard statistical methods (see the appendix), considering the fact that estimates (or the known data symbols) of I_{qn} and Q_{qn} are available. This results in

$$
\begin{bmatrix} \hat{\tilde{G}}_{qq1,n}^{cc} \\ \hat{\tilde{G}}_{qq1,n}^{sc} \end{bmatrix} = \frac{1}{(\hat{I}_{q1n})^2 + (\hat{Q}_{q1n})^2} \begin{bmatrix} r_{c1,n}^q & r_{s1,n}^q \\ r_{s1,n}^q & -r_{cn,1}^q \end{bmatrix} \begin{bmatrix} \hat{I}_{q1n} \\ \hat{Q}_{q1n} \end{bmatrix}.
\tag{12}
$$

These estimated gain samples update the phase estimate for the voltage-controlled oscillator (VCO) (see Figure 3), and generate MLE of data symbols in the following period. The phase estimate is computed as $\hat{\phi} = \tan^{-1}(\hat{\tilde{G}}_{qq1,n}^{sc}/\hat{\tilde{G}}_{qq1,n}^{cc})$.

This phase estimate can be used to correct the phase through the VCO during demodulation operation. The phase correction in turn reduces cross-rail interference.

Second stage

In this stage we recover the data in the nth interval using the gain estimate in the previous interval. We assume that we have all the signal samples available up to the nth interval and the channel gain estimates are available up to $(n-1)$th interval. The standard statistical method (see the appendix) gives

$$
\begin{bmatrix} \hat{I}_{q1,n} \\ \hat{Q}_{q1,n} \end{bmatrix}
$$
$$
= \frac{1}{(\hat{\tilde{G}}_{qq1,n-1}^{cc})^2 + (\hat{\tilde{G}}_{qq1,n-1}^{sc})^2} \begin{bmatrix} r_{c1,n}^q & r_{s1,n}^q \\ r_{s1,n}^q & -r_{c1,n}^q \end{bmatrix} \begin{bmatrix} \hat{\tilde{G}}_{qq1,n-1}^{cc} \\ \hat{\tilde{G}}_{qq1,n-1}^{sc} \end{bmatrix}.
\tag{13}
$$

Finally, a likelihood ratio test is performed to decide on the actual transmitted symbol. As observed in [8], there is a probability that this estimate can suddenly diverge from the true value. This can occur when the channel is in deep fade and the detector makes a sequence of errors resulting in a degradation of the estimates. Reinitializing the data and gain matrices periodically can alleviate this problem.

3. PERFORMANCE ANALYSIS

In this section we analyze the bit error probability for MT-CDMA signals. Here, user 1, using the qth tone in the nth sampling interval, is considered to be the user of interest. Substituting (11) into (13), we get

$$
\hat{S}(t) = \begin{bmatrix} \hat{I}_{q1,n} \\ \hat{Q}_{q1,n} \end{bmatrix} = \frac{1}{g_{n-1}} \begin{bmatrix} I_{q1,n}X_{qq1,n-1}^I + Y_{qq1,n-1}^I \\ Q_{q1,n}X_{qq1,n-1}^Q + Y_{qq1,n-1}^Q \end{bmatrix},
\tag{14}
$$

where

$$
\begin{aligned}
g_{n-1} &= (\hat{\tilde{G}}_{qq1,n-1}^{cc})^2 + (\hat{\tilde{G}}_{qq1,n-1}^{sc})^2, \\
X_{qq1,n-1}^I = X_{qq1,n-1}^Q &= \tilde{G}_{qq1,n}^{cc}\hat{\tilde{G}}_{qq1,n-1}^{cc} + \tilde{G}_{qq1,n}^{sc}\hat{\tilde{G}}_{qq1,n-1}^{sc}, \\
Y_{qq1,n-1}^I &= \frac{1}{g_{n-1}}\{Q_{q1,n}(\tilde{G}_{qq1,n}^{cc}\hat{\tilde{G}}_{qq1,n-1}^{sc} - \tilde{G}_{qq1,n}^{sc}\hat{\tilde{G}}_{qq1,n-1}^{cc}) \\
&\quad + (\eta_{c1,n}\hat{\tilde{G}}_{qq1,n-1}^{cc} + \eta_{s1,n}\hat{\tilde{G}}_{qq1,n-1}^{sc})\}, \\
Y_{qq1,n-1}^Q &= -\frac{1}{g_{n-1}}\{I_{q1,n}(\tilde{G}_{qq1,n}^{cc}\hat{\tilde{G}}_{qq1,n-1}^{sc} - \tilde{G}_{qq1,n}^{sc}\hat{\tilde{G}}_{qq1,n-1}^{cc}) \\
&\quad + (\eta_{c1,n}\hat{\tilde{G}}_{qq1,n-1}^{sc} - \eta_{s1,n}\hat{\tilde{G}}_{qq1,n-1}^{cc})\}.
\end{aligned}
\tag{15}
$$

Because of the symmetry, we can consider the in-phase branch only. In this case, the data bit estimate $\hat{I}_{q1,n}$, conditioned on the previous gain matrix $\mathbf{G}_{n-1}$ (G-terms with subscripts $n-1$), current gain matrix $\mathbf{G}_n$ (G-terms with subscripts n), and current data bit $I_{q1,n}$, is Gaussian with the

following mean and covariance, respectively:

$$E[\hat{I}_{q1,n}|\hat{\mathbf{G}}_{n-1}, \hat{\mathbf{G}}_n, I_{q1,n}] = I_{q1,n}a,$$
$$\mathrm{Cov}[\hat{I}_{q1,n}|\hat{\mathbf{G}}_{n-1}, \hat{\mathbf{G}}_n, I_{q1,n}] = b + c\sigma_n^2, \tag{16}$$

where

$$a = \frac{X_{qq1,n-1}^I}{g_{n-1}},$$

$$b = \frac{1}{(g_{n-1})^2}(\tilde{G}_{qq1,n}^{cc}\hat{\tilde{G}}_{qq1,n-1}^{sc} - \tilde{G}_{qq1,n}^{sc}\hat{\tilde{G}}_{qq1,n-1}^{cc})^2, \tag{17}$$

$$c = \frac{1}{g_{n-1}}.$$

At this stage, we perform a likelihood ratio test [17] to decide on the actual transmitted symbol. We define two hypotheses, H_0 and H_1:

$$H_0 : \hat{I}_{q1,n} = -a + Y_{qq,n-1}^{I(0)},$$
$$H_1 : \hat{I}_{q1,n} = -a + Y_{qq,n-1}^{I(1)}. \tag{18}$$

From the above hypotheses we can easily show that the likelihood ratio is proportional to $\{\hat{I}_{q1,n}/(b + c\sigma_n^2)\}$. Since b, c, and σ_n^2 are independent of the hypotheses, the test can be reduced by checking the sign of $\hat{I}_{q1,n}$ only, and we do not need to generate the estimate of σ_n^2.

The average probability of bit error, assuming that the in-phase term $\hat{I}_{q1,n} = 1$ has been transmitted, is given by

$$P(\varepsilon|\hat{I}_{q1,n})$$
$$= \int_{-\infty}^{\infty} \int_{-\infty}^{\infty} P(\varepsilon|H_1, \hat{\mathbf{G}}_{n-1}, \hat{\mathbf{G}}_n) p(\hat{\mathbf{G}}_{n-1}, \hat{\mathbf{G}}_n) d\hat{\mathbf{G}}_{n-1} d\hat{\mathbf{G}}_n, \tag{19}$$

where

$$P(\varepsilon|H_1, \hat{\mathbf{G}}_{n-1}, \hat{\mathbf{G}}_n) = \frac{1}{2}\mathrm{erfc}\left(\frac{a}{\sqrt{2(b + c\sigma_n^2)}}\right). \tag{20}$$

Substituting (20) into (19), we get

$$P(\varepsilon|I_{q1,n})$$
$$= \int_{-\infty}^{\infty} \int_{-\infty}^{\infty} \frac{1}{2} \mathrm{erfc}\left(\frac{a}{\sqrt{2(b + c\sigma_n^2)}}\right) p(\hat{\mathbf{G}}_{n-1}, \hat{\mathbf{G}}_n) d\hat{\mathbf{G}}_{n-1} d\hat{\mathbf{G}}_n. \tag{21}$$

Equation (21) does not give any closed form solution. But assuming fairly accurate gain estimation, that is,

$$\hat{\tilde{G}}_{qq1,n-1}^{cc} \approx \tilde{G}_{qq1,n}^{cc}, \qquad \hat{\tilde{G}}_{qq1,n-1}^{sc} \approx \tilde{G}_{qq1,n}^{sc}, \tag{22}$$

the solution [18] of (21) gives

$$P = \frac{1}{2}\left[1 - \left\{\frac{2\alpha_{n-1}^2 + \sigma_{n-1}^2}{2\alpha_{n-1}^2 + 2\sigma_n^2 + \sigma_{n-1}^2}\right\}^{1/2}\right], \tag{23}$$

where α_{n-1}^2 and σ_{n-1}^2 are the variances of gain terms and *noise plus interference* terms, respectively, in the $(n-1)$th time interval, while σ_n^2 represents the variance of noise plus interference in nth time interval. In this study, the assumption of slowly varying channels helps us to consider that the two consecutive noise plus interference samples differ only in the AWGN samples. We may therefore write

$$\sigma_n^2 = \sigma_{n-1}^2. \tag{24}$$

Now, we define a new term A as

$$A = \frac{\alpha_{n-1}^2}{\sigma_{n-1}^2}. \tag{25}$$

Substituting (24) and (25) into (23), we get the probability of bit error for a particular user's signal in MT-CDMA system using a particular tone q in the fading channel environment. This is given by

$$P = \frac{1}{2}\left[1 - \left(\frac{2A + 1}{2A + 3}\right)^{1/2}\right]. \tag{26}$$

To find out the numerical results from our investigations, we need to compute the expressions for α_{n-1}^2 and σ_n^2. In this case, we get two sets of expressions for Rayleigh and Ricean fading channels.

(A) α_{n-1}^2 *and* σ_n^2 *in the Rayleigh fading channel.* For the Rayleigh fading channel, we can easily show [18] that

$$\alpha_{n-1}^2 = \frac{P\rho T^2}{4}\left(1 + \frac{L-1}{3N_cN_t}\right), \tag{27}$$

$$\sigma_n^2 = \frac{P\rho T^2}{4}\left\{\frac{2(2LK - L - 1)}{3N_cN_t} + \frac{2K(2L-1)}{T^2}\right.$$
$$\left. \cdot \sum_{p=0,\neq q}^{N_t-1}\left[E\left[(R_{pq}^s)^2\right] + E\left[(R_{pq}^c)^2\right]\right] + \frac{N_0}{\overline{E}_s}\right\}. \tag{28}$$

In (28), the subscript k has been omitted from the correlation terms because the expected values of the squared correlation terms are independent of user-number k [4]. Also $\overline{E}_s = E_s\rho$ is the mean received symbol energy and ρ is the average path power, which is assumed to be constant (i.e., $\rho_{kl} = \rho$) for all the paths and users in the channel under consideration. $E_s = PT$ is the received symbol energy. Now, substituting the expressions of (27) and (28) into (26), we can evaluate the numerical results for the probability of bit error in the Rayleigh fading channel.

(B) α_{n-1}^2 *and* σ_n^2 *in the Ricean fading channel.* Here, assuming that β_{11}^2, the variance of the first path for user 1, is known, we get the expression of α_{n-1}^2 as [19]

$$\alpha_{n-1}^2 = \frac{P\beta_{11}^2 T^2}{4} + \frac{P(S^2 + 2\sigma_r^2)T^2(L-1)}{12N_cN_t}, \tag{29}$$

where the terms S^2 and $2\sigma_r^2$ have already been defined in Section 2.2. Defining a new variable

$$\psi = \frac{\beta_{11}^2}{S^2 + 2\sigma_r^2}, \tag{30}$$

we get

$$\alpha_{n-1}^2 = \frac{PT^2(S^2 + 2\sigma_r^2)}{4}\left(\psi + \frac{L-1}{3N_cN_t}\right). \qquad (31)$$

The expression for σ_n^2 becomes

$$\sigma_n^2 = \frac{PT^2(S^2 + 2\sigma_r^2)}{4}$$
$$\times \left\{ \frac{2(2LK - L - 1)}{3N_cN_t} + \frac{2K(2L-1)}{T^2} \right. \qquad (32)$$
$$\left. \cdot \sum_{p=0,\neq q}^{N_t-1}\left[E\left[\left(R_{pq}^s\right)^2\right] + E\left[\left(R_{pq}^c\right)^2\right]\right] + \frac{N_0}{\overline{E_s}}\right\}.$$

In (32), the subscript k has been omitted from the correlation terms for the same reason mentioned earlier. Here, $\overline{E_s} = E_s(S^2 + 2\sigma_r^2)$ is the mean received symbol energy. The average path power $(S^2 + 2\sigma_r^2)$ is assumed to be constant for all the paths and users (except for the power associated with the first user in the first path, i.e., β_{11}^2) in the channel under consideration. $E_s = PT$ is the received symbol energy.

Now that the expression of α_{n-1}^2 is derived assuming that β_{11}^2, or in other words ψ, is known, (26) becomes the expression for the conditional BER as

$$P(e|\psi) = \frac{1}{2}\left[1 - \left(\frac{2A+1}{2A+3}\right)^{1/2}\right]. \qquad (33)$$

In this case, to find out the probability of BER of our interest, we need to average (33) over the PDF of ψ. Since β_{11} is a Ricean distributed random variable, consequently, ψ is a normalized noncentral chi-squared random variable. The PDF of ψ can easily be derived [18] as

$$p(\psi) = (R+1)\exp\left[-\{R + \psi(R+1)\}\right]$$
$$\times I_0\left[2\{\psi R(R+1)\}^{1/2}\right]. \qquad (34)$$

Finally, the expression for the average bit error probability in the Ricean fading channel becomes

$$P(e) = \int_0^\infty P(e|\psi)p(\psi)d\psi. \qquad (35)$$

Now substituting the expressions of (30), (32), (33), and (34) into (35), we can evaluate the numerical results for the probability of bit error in the Ricean fading channel. In this case, the integration in (35) does not give any closed-form solution and that is why we perform numerical integration for our results.

4. NUMERICAL RESULTS AND DISCUSSION

In this section, we present some numerical results in terms of BER. In all calculations, a channel with four paths has been used. The maximum number of tones used here is 32. The overall BW is assumed to be constant. To guarantee constant BW, identical chip duration is ensured with constant ratio between the number of chips and the number of tones. This
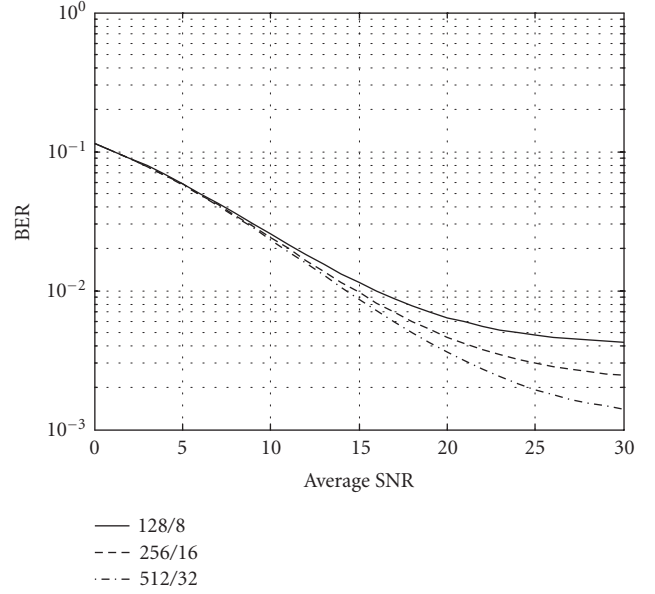

FIGURE 4: BER performance in the Rayleigh fading channel for PN-code length and tones ratio, $N_c/N_t = 128/8 = 256/16 = 512/32$ in the presence of single user.

can be further explained. With single-tone symbol duration T and the number of chips in the spreading sequence N_c, for N_t number of tones, the symbol duration becomes N_tT and the total number of chips becomes N_tN_c. As a result, identical chip duration $T_c = T/N_c = N_tT/N_tN_c$ or, in other words, constant BW $(\cong 1/T_c)$ is ensured. We have kept a constant delay range irrespective of the number of tones and this delay range is equal to the symbol duration corresponding to single-tone transmission.

Identical considerations have been made in [4] for coherent MT-CDMA system's performance study. This permits us to compare the performance of the TSMLE-based MT-CDMA system to the results reported in [4] for the Ricean fading channel. While computing the BER analytically, it has been found that the signal transmitted by the tone (e.g., q) positioned at the center of the spectrum (of all N_t tones) provides worst-case performance. This is due to the cross carrier interference by which the central tone is mostly affected compared to the other tones. This worst-case scenario has been considered in all the analytical results.

Here, Figures 4, 5, and 6 show the performances of the TSMLE-based MT-CDMA system in terms of BER in Rayleigh fading channel while Figures 7 and 8 show the performance in Ricean fading channel. Finally, Figure 9 shows a BER performance comparison between TSMLE-based MT-CDMA and coherent MT-CDMA systems with identical setting. In Figure 4, BER versus the averaged received symbol energy over noise ratio (SNR) for single user case is plotted for the Rayleigh fading channel. There is no interfering user. The curves clearly show that, with an increase in the number of tones, performance of the system improves in terms of BER. In the performance curves, the irreducible error
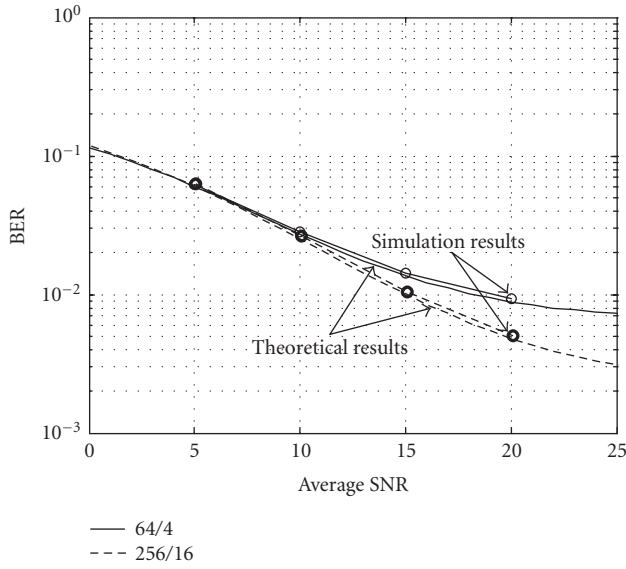
FIGURE 5: Theoretical and simulation results for TSMLE-based MT-CDMA system in the Rayleigh fading channel without the presence of MAI. Number of paths-4.
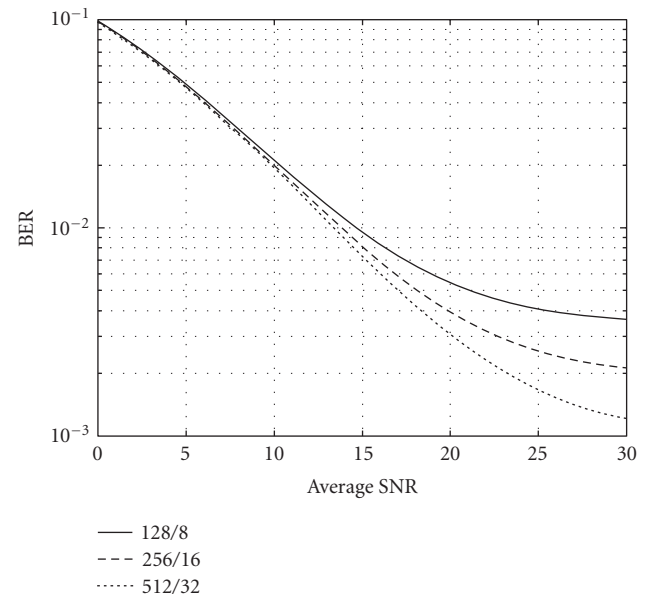

FIGURE 7: BER performance in the Ricean fading channel ($R = 2$) for PN-code length and tones ratio, $N_c/N_t = 128/8 = 256/16 = 512/32$ in the presence of single user.
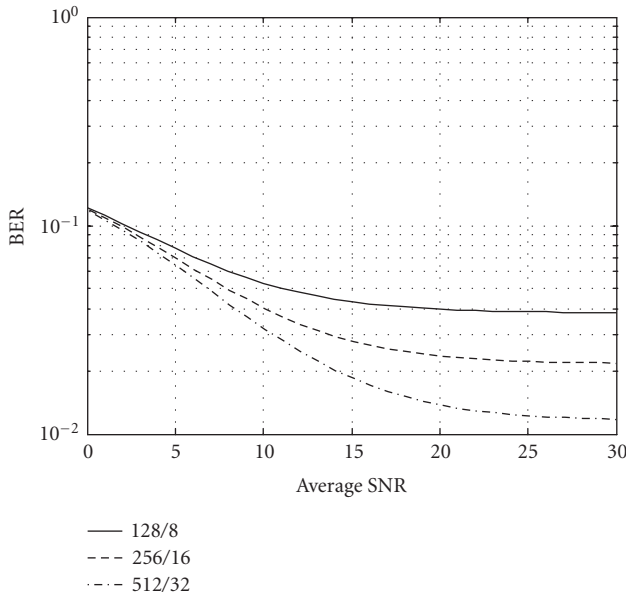

FIGURE 6: BER performance in the Rayleigh fading channel for PN-code length and tones ratio, $N_c/N_t = 128/8 = 256/16 = 512/32$ in the presence of MAI (10 users).
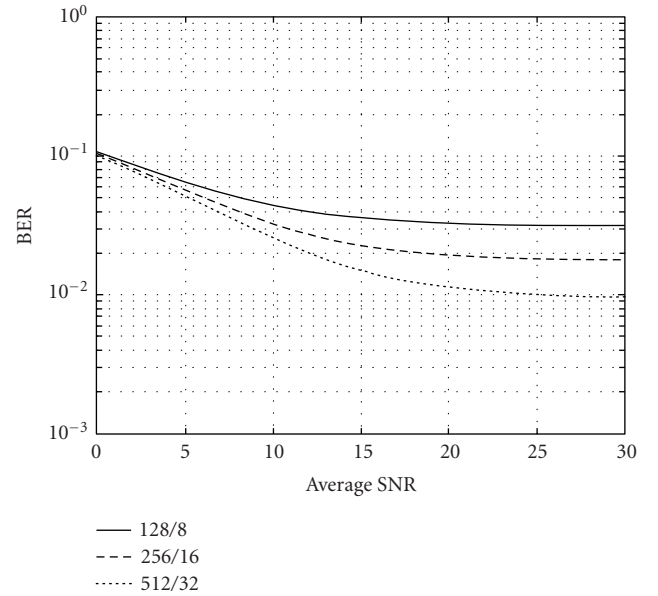

FIGURE 8: BER performance in the Ricean fading channel ($R = 2$) for PN-code length and tones ratio, $N_c/N_t = 128/8 = 256/16 = 512/32$ in the presence of MAI (10 users).

probability is encountered due to the presence of ISI and ICI (for $N_t > 2$), which are not cancelled at the receiver. It is interesting to note that with higher number of tones, this irreducible error floor is notably reduced. This can be explained by the fact that as we increase the number of tones in the system, the symbol duration becomes larger, which in turn makes the effect of ISI smaller on the BER performance. On the other hand, as we are always considering the central fre-

quency ($q = N_t/2$) for the analysis, the ICI, resulting from the reasonable increase in the number of tones, does not increase significantly. In this case, the tones sitting around both edges of the MT-spectrum have little effect on the central frequency, the carrier frequency of interest. So, at higher number of tones, with a considerable decrease in the ISI and very small increase in the ICI, the overall effect of the interference becomes smaller, making the error floor significantly low.
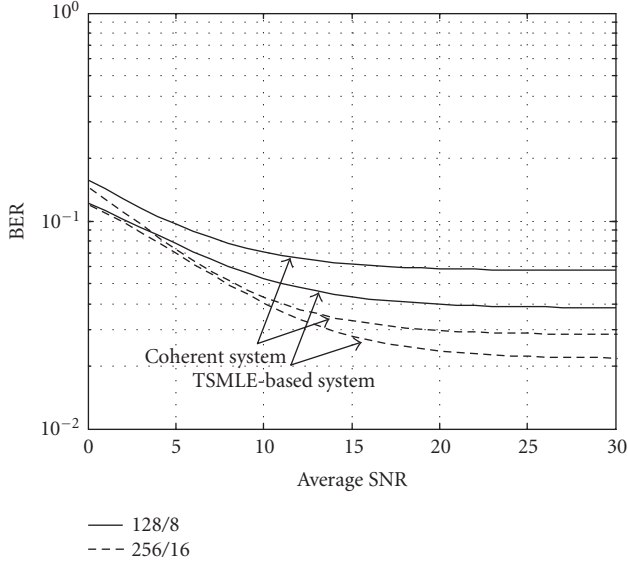
Figure 9: Comparison of BER performance between TSMLE-based MT-CDMA system and coherent MT-CDMA system [4] with identical study scenario. The Ricean parameter $R = 1$, the number of paths is 4, the number of users is 10, and the delay range is constant with the PN-code length and tones ratio, $N_c/N_t = 128/8 = 256/16$.

Figure 5 shows the results for the theoretical and the simulated BER performances in terms of average SNR for a single user case (no MAI) over a Rayleigh fading channel. The results show very close agreement between theory and simulation. In the simulation, we have considered Rayleigh distributed four-path channel model. The simulation results have been obtained by averaging over one million samples of 200 independent runs. We have used *Hadamard code* for PN sequences and have not considered any Doppler effect in our simulations. In the simulations we have assumed a delay range of 200 nanoseconds resulting in a highest bit rate of 10 Mbps for the QPSK-modulation-based MT-CDMA system.

Figure 6 shows the BER as a function of SNR, obtained in a Rayleigh fading channel for a particular user, in the presence of multiple users. A total number of 10 users is considered in this set-up. Here, due to the presence of MAI, the overall performance is worse than the single-user performance. The performance shows that even in the presence of MAI, a gain in the BER can be achieved for larger number of tones. The system performance exhibits irreducible error probability even at higher number of tones. In this case, although at higher number of tones, (as discussed earlier) the ICI does not increase significantly, and the effect of the ISI is greatly reduced; the MAI provides a major detrimental role on the system's performance. Here, at higher SNR, the MAI cannot be compensated due to the presence of the interfering users transmitting their signals with equal power, and as a result, at higher SNRs the MAI keeps the error floor approximately unchanged.

In case of Ricean fading channel, all the results are obtained using numerical integration with Ricean parameter

$R = 2$. Figure 7 shows the BER versus the SNR obtained for a single-user case in the absence of MAI. The performance curves show that as we increase the number of tones, we get performance improvements. As seen in Figure 4 for Rayleigh fading channel, here, we also encounter error floors for lower number of tones that get significantly reduced with the increase in the number of tones. The reason of reduced error floor at higher number of tones carries the same explanation as has been stated for the Rayleigh fading case.

Figure 8 shows the BER as a function of SNR, for an arbitrary user (here, user 1), obtained in the presence of multiple users. As before, a total number of 10 users is considered here. The performance curves show similar characteristics as shown in Figure 6 for Rayleigh fading channel. If we compare the performance of the system in the Ricean fading channel with that in the Rayleigh fading one, we observe that the former one performs better due to the presence of a strong path in its multipath components.

For the Ricean fading channel, the comparison with the QPSK-modulation-based coherent MT-CDMA system [4] shows (Figure 9) that at lower number of tones (8 tones) the TSMLE-based system performs better (approximately 5 dB at a BER of 8×10^{-2}) than its coherent counterpart. At higher number of tones, this performance gain over the coherent system becomes reduced, which can be explained as follows. The performance gain over coherent system results due to the ML estimations of channel gains and data symbols. While estimating the phase from the channel gain functions, we assume that all the phase variations in the multipath components of the desired signal are constant (equation (10)) and we use this estimated phase to fix the VCO at the front end of the receiver. In actual circumstances, all these phases are varying to some extent. With small number of tones this consideration has negligible effect on the performance gain while with higher number of tones, in the presence of all the interferences (ICI, MAI, cross rail interference, etc.), this consideration results in smaller gain improvement. Consequently, at lower number of tones the performance gain of the TSMLE-based system is higher than the coherent system, while at higher number of tones it is smaller. As a whole, the results show that we can get better BER performance of the TSMLE-based MT-CDMA system compared to the coherent case without taking into account the phase-tracking mechanism, which is considered to be one of the most complex functions in the system.

In all the performance curves, it is observed that the increase in gain, going from 8 to 16 tones is greater than going from 16 to 32 tones. This shows that gain saturation in the BER performance is encountered as the number of tones increases. This can be explained in the following way. With the increase in the number of tones, the transmitted symbol duration gets increased in the time domain, which is equivalent to sending the same symbol (corresponding to single tone) in different consecutive time slots. Consequently, an inherent diversity takes place during transmission. In case of diversity combining, with independent fading in each time slot, if the probability of a signal in error (i.e., the signal will fade below a certain level) in one time slot is p, then it becomes p^M for

M different independent time slots. As a result, the probability of a signal not in error will be equal to $(1 - p^M)$, which shows that with the increase in the time slots (i.e., with the increase in the MT symbol duration) that results from the increase in the number of tones, the performance gain starts to saturate.

In the practical setting, in increasing the number of tones, we need to take into account the system complexity and MT symbol length. With the increase in the number of tones, we need fast Fourier transform (FFT) and inverse FFT (IFFT) operators of larger sizes, which in turn make the system more complex. On the other hand, with the increase in the symbol length with higher number of tones, the channel might not be slow any more, and that will produce some unrealistic results. Thus the upper limit of number of tones depends on two factors: the type of the channel and the target bit rate.

There are many challenges, which are not considered in the limited scope of this paper. Working with MT-CDMA system, which is an OFDM-based system, gives two substantial challenges. Firstly, due to the large dynamic range of the output of the FFT, OFDM has a larger peak-to-average power ratio (PAPR) compared to single-carrier systems. This reduces the power efficiency and increases the cost of the power consumption of the transmitter amplifier. Secondly, OFDM system is susceptible to frequency offset and phase noise. In future, these challenges, including the challenge in the reduction of the various interferences such as MAI, ISI, and ICI, need to be addressed in the area of 3G wireless systems using MT-CDMA scheme.

5. CONCLUSIONS

In this paper we have proposed a TSMLE-based receiver for MT-CDMA system. This receiver can be considered as a partially coherent receiver. An analytical technique for determining the BER performance of MT-CDMA system with its proposed receiver structure has been presented. The study has considered indoor environment with both Rayleigh and Ricean fading channels. The influence of the number of tones has been shown for a constant delay range. Different combinations of code lengths and number of tones have been considered under a constrained bit rate. The numerical results in the Ricean fading channel show that TSMLE-based MT-CDMA receiver performs better than fully coherent MT-CDMA system. Although the analytical method presented in this paper has been developed for indoor channel environment, this method can be applied for any other type of channels with little modifications.

APPENDIX

A. MAXIMUM LIKELIHOOD (ML) GAIN AND DATA ESTIMATES

In this appendix we derive the expressions of ML gain and data estimates for MT-CDMA signals. Here, the quadrature received signal samples r_{cn} and r_{sn} in an nth time interval are given by

$$
\begin{aligned}
r_{cn} &= I_n G_{cn} - Q_n G_{sn} + \eta_{cn}, \\
r_{sn} &= I_n G_{sn} + Q_n G_{cn} + \eta_{sn},
\end{aligned}
\tag{A.1}
$$

where I_n and Q_n are the nth samples of the quadrature data components, G_{cn} and G_{sn} are the nth samples of the quadrature gain components and, η_{cn} and η_{sn} are the nth samples of the quadrature noise plus interference components. η_{cn} and η_{sn} components are considered to be Gaussian distributed random variables.

A.1. ML gain estimates

Since η_{cn} and η_{sn} samples are Gaussian distributed random variables, so if we assume that all the data and gain samples are known, the received signal components are also Gaussian distributed random variables. The first task is to determine the conditional means and variances of the received signal samples, given $\{I_n, Q_n, G_{cn}, G_{sn}\}$. The conditional means are

$$
\begin{aligned}
m_1 &= E(r_{cn}|I_n, Q_n, G_{cn}, G_{sn}) = I_n G_{cn} - Q_n G_{sn}, \\
m_2 &= E(r_{sn}|I_n, Q_n, G_{cn}, G_{sn}) = I_n G_{sn} + Q_n G_{cn}.
\end{aligned}
\tag{A.2}
$$

In (A.2), $E(x)$ represents the expected value of x. The quadrature received signal samples have an identical variance of σ_r^2 given by

$$
\sigma_r^2 = \text{Var}(r_{cm}) = \text{Var}(r_{sm}).
\tag{A.3}
$$

In (A.3), $\text{Var}(x)$ represents the variance of x. Since the quadrature components are statistically independent, of each other so the joint PDF of the two received data samples conditioned on the available quadrature data estimates (or known data) and gains are given by

$$
\begin{aligned}
&p(r_{cn}, r_{sn}|\hat{I}_n, \hat{Q}_n, G_{cn}, G_{sn}) \\
&= \frac{1}{2\pi\sigma_r^2} \exp\left[-\left\{\frac{(r_{cn} + m_1)^2}{2\sigma_r^2} + \frac{(r_{sn} + m_2)^2}{2\sigma_r^2}\right\}\right],
\end{aligned}
\tag{A.4}
$$

where $\hat{I}_n$ and $\hat{O}_n$ are the estimated quadrature data components. The gain estimates are selected to minimize the log likelihood function. Taking natural log on both sides of (A.4), we get

$$
\begin{aligned}
&\log\left[p(r_{cn}, r_{sn}|\hat{I}_n, \hat{Q}_n, G_{cn}, G_{sn})\right] \\
&= \log\left[\frac{1}{2\pi\sigma_r^2}\right] - \left\{\frac{(r_{cn} + m_1)^2}{2\sigma_r^2} + \frac{(r_{sn} + m_2)^2}{2\sigma_r^2}\right\}.
\end{aligned}
\tag{A.5}
$$

Now, letting the estimate of G_{cn} be G_{cn} and taking the derivative of (A.5) with respect to G_{cn} and equating it to zero, we get

$$
\hat{G}_{cn} = \frac{r_{cn}\hat{I}_n + r_{sn}\hat{Q}_n}{\hat{I}_n^2 + \hat{Q}_n^2}.
\tag{A.6}
$$

Similarly, letting the estimate of G_{sn} be $\hat{G}_{sn}$ and taking the derivative of (A.5) with respect to G_{sn} and equating it to zero, we get

$$\hat{G}_{sn} = \frac{r_{sn}\hat{I}_n - r_{cn}\hat{Q}_n}{\hat{I}_n^2 + \hat{Q}_n^2}. \tag{A.7}$$

Equations (A.6) and (A.7) can be represented in the matrix form as given below:

$$\begin{pmatrix} \hat{G}_{cn} \\ \hat{G}_{sn} \end{pmatrix} = \frac{1}{\hat{I}_n^2 + \hat{Q}_n^2} \begin{pmatrix} r_{cn} & r_{sn} \\ r_{sn} & -r_{cn} \end{pmatrix} \begin{pmatrix} \hat{I}_n \\ \hat{Q}_n \end{pmatrix}. \tag{A.8}$$

A.2. ML data estimates

In this stage we recover the data in the nth interval using the gain estimates in the previous interval. We assume that we have all the signal samples available up to the nth interval and the channel gain estimates are available up to $(n-1)$th interval. Since we are considering a very slow varying channel, we can replace G_n terms with G_{n-1} terms in (A.5). The data estimates are selected to minimize the log likelihood function with G_{n-1} replacing G_n.

Taking derivative of (A.5) with respect to Q_n and equating it to zero, we get the estimate of I_n as

$$\hat{I}_n = \frac{r_{sn}\hat{G}_{s,n-1} + r_{cn}\hat{G}_{c,n-1}}{\hat{G}_{c,n-1}^2 + \hat{G}_{s,n-1}^2}. \tag{A.9}$$

Taking derivative of (A.5) with respect to Q_n and equating it to zero, we get the estimate of Q_n as

$$\hat{Q}_n = \frac{r_{sn}\hat{G}_{c,n-1} - r_{cn}\hat{G}_{s,n-1}}{\hat{G}_{c,n-1}^2 + \hat{G}_{s,n-1}^2}. \tag{A.10}$$

Formulas (A.9) and (A.10) may be written in matrix form as

$$\begin{pmatrix} \hat{I}_n \\ \hat{Q}_n \end{pmatrix} = \frac{1}{\hat{G}_{c,n-1}^2 + \hat{G}_{s,n-1}^2} \begin{pmatrix} r_{cn} & r_{sn} \\ r_{sn} & -r_{cn} \end{pmatrix} \begin{pmatrix} \hat{G}_{c,n-1} \\ \hat{G}_{s,n-1} \end{pmatrix}. \tag{A.11}$$

REFERENCES

[1] T. S. Rappaport, R. M. Annamalai, A. Buehrer, and W. H. Tranter, "Wireless communications: past events and a future perspective," *IEEE Communications Magazine*, vol. 40, no. 5, pp. 148–161, 2002.

[2] M. Ibnkahla, Q. M. Rahman, A. I. Sulyman, H. A. Al-Asady, J. Yuan, and A. Safwat, "High-speed satellite mobile communications: technologies and challenges," *Proceedings of the IEEE*, vol. 92, no. 2, pp. 312–339, 2004.

[3] S. Hara and R. Prasad, "Overview of multicarrier CDMA," *IEEE Communications Magazine*, vol. 35, no. 12, pp. 126–133, 1997.

[4] L. Vandendorpe, "Multitone spread spectrum multiple access communications system in a multipath Rician fading channel," *IEEE Trans. Vehicular Technology*, vol. 44, no. 2, pp. 327–337, 1995.

[5] S. Ohmori, Y. Yamao, and N. Nakajima, "The future generations of mobile communications based on broadband access technologies," *IEEE Communications Magazine*, vol. 38, no. 12, pp. 134–142, 2000.

[6] A. B. Sesay, "Two-stage maximum likelihood estimation for diversity combining in digital mobile radio," *IEEE Trans. Communications*, vol. 40, no. 4, pp. 676–679, 1992.

[7] R. Haeb and H. Meyr, "A systematic approach to carrier recovery and detection of digitally phase modulated signals of fading channels," *IEEE Trans. Communications*, vol. 37, no. 7, pp. 748–754, 1989.

[8] P. Kam and C. Teh, "Reception of PSK signals over fading channels via quadrature amplitude estimation," *IEEE Trans. Communications*, vol. 31, no. 8, pp. 1024–1027, 1983.

[9] A. B. Sesay, "Adaptive two-stage maximum likelihood estimation for cellular radio," *IEE Proceedings-Communications*, vol. 141, no. 1, pp. 39–48, 1994.

[10] S. Sampei and T. Sunaga, "Rayleigh fading compensation method for 16 QAM in digital land mobile radio channels," in *IEEE 39th Vehicular Technology Conference (VTC '89)*, pp. 640–646, San Francisco, Calif, USA, May 1989.

[11] A. Aghamohammadi, H. Meyr, and G. Ascheid, "A new method for phase synchronization and automatic gain control of linearly modulated signals of frequency-flat fading channels," *IEEE Trans. Communications*, vol. 39, no. 1, pp. 25–29, 1991.

[12] P. Kam and C. Teh, "An adaptive receiver with memory for slowly fading channels," *IEEE Trans. Communications*, vol. 32, no. 6, pp. 654–659, 1984.

[13] A. Aghamohammadi and H. Meyr, "On the error probability of linearly modulated signals on Rayleigh frequency-flat fading channels," *IEEE Trans. Communications*, vol. 38, no. 11, pp. 1966–1970, 1990.

[14] P. Varshney and A. Haddad, "A receiver with memory for fading channels," *IEEE Trans. Communications*, vol. 26, no. 2, pp. 278–283, 1978.

[15] P. K. Frenger, N. Arne, and B. Svensson, "Decision-directed coherent detection in multicarrier systems on Rayleigh fading channels," *IEEE Trans. Vehicular Technology*, vol. 48, no. 2, pp. 490–498, 1999.

[16] H. Hashemi, "The indoor radio propagation channel," *Proceedings of the IEEE*, vol. 81, no. 7, pp. 943–968, 1993.

[17] J. G. Proakis, *Digital Communications*, McGraw Hill, New York, NY, USA, 3rd edition, 1995.

[18] Q. M. Rahman, *Performance Analysis of MT-CDMA System*, Ph.D. dissertation, University of Calgary, Calgary, Alberta, Canada, 2002.

[19] Q. M. Rahman and A. B. Sesay, "MT-CDMA system with two stage maximum likelihood symbol estimation," in *IEEE 56th Vehicular Technology Conference (VTC '02)*, vol. 1, pp. 539–543, Vancouver, British Columbia, Canada, September 2002.

Quazi Mehbubar Rahman received the B.S. and M.S. degrees in applied physics and electronics from the University of Dhaka, Bangladesh in 1990 and 1992, respectively, and the Ph.D. degree in electrical engineering from the University of Calgary, Canada in 2002. From 1993 to 1996, he was with the Department of Applied Physics & Electronics at the University of Dhaka as a Lecturer. From 1997 to 2001 he served as a research associate in the Department of Electrical & Computer Engineering, University of Calgary. Since 2002, he has been with Queen's University, Canada, where he is currently a Postdoctoral Fellow in the Department of Electrical & Computer Engineering. Currently, Dr. Rahman is holding a Visiting Professor position in the Department of Electrical and Computer Engineering, Royal Military

College of Canada. Dr. Rahman is a contributing author to *Signal Processing for Mobile Communications Handbook* (2004), and to a good number of journal and conference papers in the areas of wireless communications. He is a recipient of the Canadian Commonwealth Scholarship. His research interest includes spread spectrum and MIMO systems, OFDM systems, and channel coding, estimation, and detection in the area of wireless mobile and satellite communications.

Abu B. Sesay received the Ph.D. degree in electrical engineering from McMaster University, Hamilton, ON, Canada, in 1988 where he also worked as a Research Associate from 1986 to 1989. He worked on various ITU (International Telecommunications Union) projects from 1979 to 1984. In 1989, he joined the University of Calgary where he is now a Full Professor and Associate Head. He has been involved with TRLabs, Canada, since 1989, where he is now a TRLabs Adjunct Scientist. His current research activities include space-time coding, MC-CDMA, multiuser detection, equalization, error correction coding, MIMO systems, optical fiber/wireless communications, and adaptive signal processing. Dr. Sesay is the recipient of the IEEE 1996 Neal Shepherd Memorial Best Propagation Paper Award. He is also the recipient of the Departmental Research Excellence Award for 2002. His students have received three IEEE conference best paper awards.

Mostafa Hefnawi received the Ph.D. degree in electrical engineering from Laval University, Quebec, in 1998. He is currently an Associate Professor in the Department of Electrical and Computer Engineering of the Royal Military College of Canada. His research interests are in the areas of WCDMA wireless communication, smart antenna techniques, and MIMO systems.